Open Archive Toulouse Archive Ouverte (OATAO)

OATAO is an open access repository that collects the work of Toulouse researchers and makes it freely available over the web where possible.

To link to this article:
 URL: http://dx.doi.org/10.1016/j.elecom.2009.11.017

Combining phosphate species and stainless steel cathode to enhance hydrogen evolution in microbial electrolysis cell (MEC)

Leonardo DeSilva Munoz [1], Benjamin Erable, Luc Etcheverry, Julien Riess, Régine Basséguy, Alain Bergel *

Laboratoire de Génie Chimique, CNRS – Université de Toulouse, 4 Allée Emile Monso, 31432 Toulouse, France

A B S T R A C T

Microbial electrolysis cells (MEC) must work around neutral pH because of microbial catalysis at the anode. To develop a hydrogen evolution cathode that can work at neutral pH remains a major challenge in MEC technology. Voltammetry performed at pH 8.0 on rotating disk electrodes showed that the presence of phosphate species straightforwardly multiplied the current density of hydrogen evolution, through the so-called cathodic deprotonation reaction. The mechanism was stable on stainless steel cathodes whereas it rapidly vanished on platinum. The phosphate/stainless steel system implemented in a 25 L MEC with a marine microbial anode led to hydrogen evolution rates of up to 4.9 L/h/m^2 under 0.8 V voltage, which were of the same order than the best performance values reported so far.

## 1. Introduction

Hydrogen gas can be produced by the electrolysis of organic matter in a so-called microbial electrolysis cell (MEC) [1,2]. In a MEC, the evolution of hydrogen at the cathode is the same as for traditional water electrolysis:

$$2H^+ + 2e^- \rightarrow H_2$$
$$E^0_{H^+/H_2} = 0.0 - 0.059pH/SHE \tag{1}$$
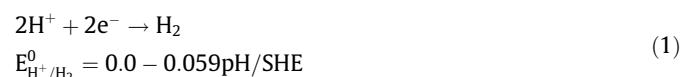
while, at the anode, the oxidation of water is replaced by the oxidation of organic compounds, generally acetate, which is converted to bicarbonate:

$$CH_3COO^- + 4H_2O \rightarrow 2HCO_3^- + 9H^+ + 8e^-$$
$$E^0_{HCO_3^-/CH_3COO^-} = 0.187 - 0.066pH \text{ V/SHE[3]} : \tag{2}$$
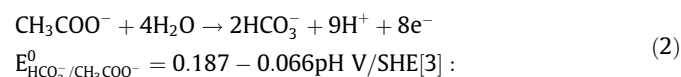
This oxidation is catalysed by a microbial biofilm that forms on the anode surface and plays the role of an electrocatalyst [4]. Comparing the thermodynamic equilibrium of this system, 0.236 V (at pH 7.0), to the 1.23 V required for water electrolysis evidences the promising potential of MEC technology. Performance has progressed remarkably in only a few years and production rates have been assessed to be as high as 3.12 m^3/m^3/day (see [3] and [5] for review). Nevertheless, designing efficient cathode for MEC remains a serious challenge. The microbial anodes used in MECs need the cell to work around neutral pH values, at which the traditional H$_2$-evolving cathodes (nickel alloys for alkaline electrolysis (pH > 14) or platinum-based catalysts for acidic electrolysis (pH < 1)) lose most of their catalytic efficiency [2]. Recent studies have looked for new H$_2$-evolving catalysts able to work at neutral pH, such as tungsten carbide [6] or nickel oxide coating [7] and they have brought to light the interest of stainless steel [8].

The presence of phosphate species and other weak acids has recently been shown to have a beneficial effect in MEC, because the charged species increase the electrolyte conductivity and also reduce the overpotential on Pt-graphite cathodes [9]. Our previous work on microbial corrosion showed that phosphate species undergo cathodic deprotonation on stainless steel, resulting in an enhancement of the hydrogen evolution reaction [10,11]. The purpose of the present work was to determine whether the cathodic deprotonation of phosphate identified in corrosion could be exploited to enhance H$_2$ production in neutral-pH electrolysis. The cathode was tested in a MEC that used a microbial anode formed from marine sediment and operated at high salinity.

2. Materials and methods

2.1. Voltammetry

The rotating disk electrodes (RDE) made of platinum (2 mm diameter) or AISI 316 L stainless steel (5 mm diameter) embedded in Teflon® were polished with a 1 μm grade abrasive sheet (3 M imperial) and ultrasonically cleaned in deionised water before each experiment. A platinum grid was used as auxiliary electrode and a saturated calomel electrode (SCE, −0.241 V/SHE) as reference

(Radiometer Analytical). Experiments were performed in a 100 mL Metrohm cell at room temperature. A nitrogen flow was maintained above the solution throughout the experiments. Potential scans (20 mV s^{-1}) started from −0.1 V/SCE for platinum and from −0.5 V/SCE for stainless steel.

2.2. Microbial electrolysis cell

A calibration curve (hydrogen flow rate *versus* current) was recorded under galvanostatic conditions (Biologic SA potentiostat) in the 0–60 A/m^2 range with a flat 254SMO stainless steel plate in a cathode compartment closed and fitted with an outlet pipe linked to a flowmeter. The electrode was cleaned by 20 min immersion in 2–20% fluoridric/nitric acid solution.

The anode compartment of the MEC was a 20 cm diameter cylinder of Plexiglas containing 25 L seawater at pH 7.5 added with marine sediments from the Atlantic Ocean. It was equipped with a cylindrical felt carbon anode (Le Carbone Loraine) of 0.25 m^2 projected surface area. It was regularly fed with sodium acetate to ensure a concentration around 10 mM. The anode was polarized at −0.1 V/SCE to form an efficient electro-active biofilm as described previously [12]. After 15 days' polarization, the microbial anode sustained a stable current density about 2.0 A/m^2 for some weeks. The cathode compartment was a 6-cm-diameter coaxial cylinder equipped with a cationic exchange membrane (Ultrex CMI-7000 Membranes Int. Inc.) set up on three lateral windows of 30 cm^2 each. The cathode compartment filled with 0.85 L water containing 0.5 M sodium phosphate pH 8.0 worked in batch mode at room temperature. The cathode was made up of two 254SMO flat stainless steel electrodes of 25 cm^2 projected surface area each. Potentials were measured *versus* a SCE electrode placed in the anode compartment.

3. Results and discussion

3.1. Voltammetry

Voltammery was performed with platinum (Fig. 1A) and stainless steel (Fig. 1B) disk electrodes rotating at 1000 rpm using different phosphate concentrations at pH 8.0, with 0.1 M KCl as the supporting electrolyte. The presence of 0.1 M KCl ensured that ionic migration was not rate-limiting, consequently the effect of different concentrations of charged species cannot be attributed to an effect on conductivity. Reduction waves started at around −0.7 V/SCE with platinum and −0.9 V/SCE for stainless steel, and the current density increased with the concentration of phosphate. A current density higher than 100 A/m^2 was reached at −0.85 V/SCE on platinum with 0.5 M phosphate, while less than 5 A/m^2 was obtained in the supporting electrolyte only. Current density values at a given potential showed a linear relationship with phosphate concentration (insets of Fig. 1). All experiments were performed at the same pH value, and the 0.1 M supporting electrolyte avoided any limitation by ion migration.

The dependence of current on phosphate concentration is explained by the electrochemical deprotonation of phosphate that has been identified previously in the field of corrosion [10,11]. Phosphate species can loose a hydrogen atom by direct reduction on the electrode surface:

$$H_2PO_4^- + e^- \rightarrow HPO_4^{2-} + 1/2H_2 \tag{3}$$

This reaction produces hydrogen and the acid–base equilibrium that follows:

$$HPO_4^{2-} + H_2O \rightarrow H_2PO_4^- + OH^- \tag{4}$$

results in the catalysis of hydrogen evolution on the material surface:
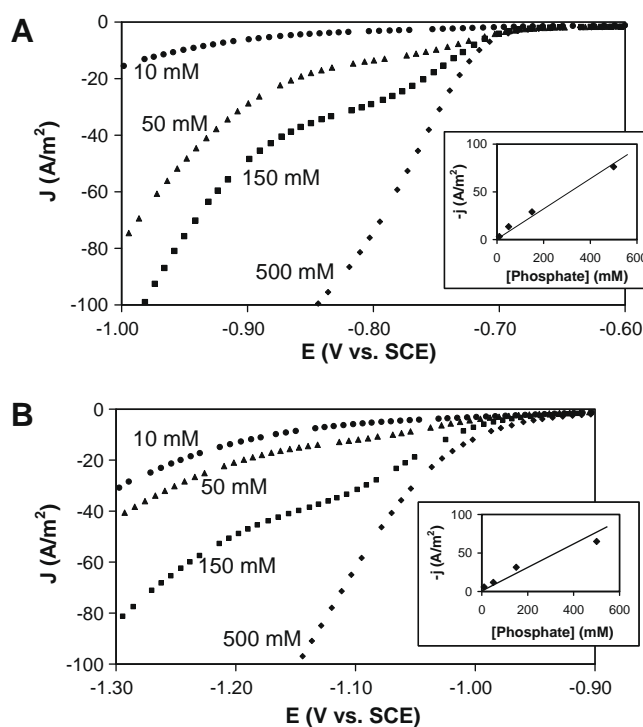

Fig. 1. Voltammetry (20 mV/s) on RDE (1000 rpm) in a pH 8.0 solution containing 0.1 M KCl and different concentrations of phosphate. (A) platinum electrode; (B) stainless steel electrode; in insets, current density at −0.80 V/SCE (platinum) or −1.10 V/SCE (stainless steel) as a function of phosphate concentration.

$$H_2O + e^- \rightarrow 1/2H_2 + OH^- \tag{5}$$

It is worth noting that this mechanism assumes that the phosphate species itself ($H_2PO_4^-$ and HPO_4^{2-}) undergoes direct reduction on the electrode surface. It should be mentioned that this scheme is different from deprotonation followed by reduction of the proton produced.

It is known that the presence of buffer can increase the hydrogen evolution current by enhancing the transport of H$^+$ towards the electrode surface. In this case, it is assumed that the transport of the buffer (protonated species) adds to the transport of proton, but the reactive compound remains the proton only and the concentration of proton at the electrode surface cannot exceed 10^{-8} M (pH 8). Here it is not possible to assume that current density up to 100 A/m^2 was obtained with a concentration of reactant of 10^{-8} M on the electrode surface; consequently, the reactant must be different from H$^+$. It has been demonstrated that the reactive was the protonated species itself [10,11,13]. Phosphate species act on stainless steel as a homogeneous catalyst of hydrogen evolution. Several weak acids have been shown to be able to give a reduction wave at potentials that increase with their dissociation constant [13]. Here $H_2PO_4^-$, with a higher dissociation constant ($10^{-7.21}$) should be easier to reduce than HPO_4^{2-} ($10^{-12.33}$) [14]. Consequently $H_2PO_4^-$ should logically correspond to the first wave observed. HPO_4^{2-}, which was the predominant species at pH 8.0 (86% of total phosphate) should be responsible for the larger current increase observed at more negative potentials.

Voltammetry curves were recorded successively in 0.5 M phosphate, 0.1 KCl solution, pH 8.0. The electrodes were disconnected and the solution was stirred for a few minutes between each curve. On platinum, the current–potential curves were drastically shifted towards negative potentials from one scan to the next (Fig. 2). The current potential-curve recorded during the first scan was fully recovered when the experiment was repeated after cleaning the
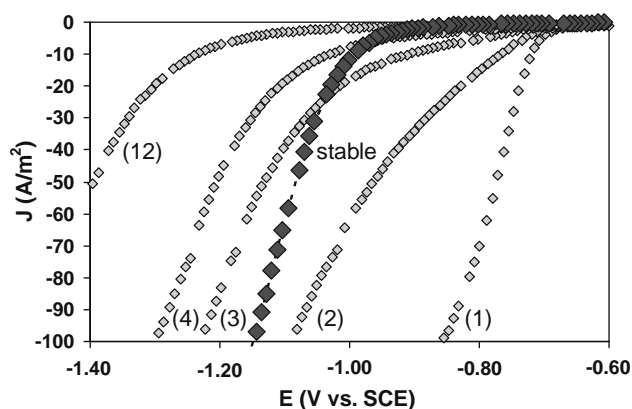
Fig. 2. Successive potential scans (20 mV/s) on platinum (grey diamonds) and stainless steel (black diamonds) RDE (1000 rpm) in pH 8.0 solution containing 0.1 M KCl and 0.5 M phosphate. The number of the potential scan is indicated on each curve.

platinum electrode. In contrast, the successive scans performed with stainless steel gave fully identical current–potential curves. No variation was observed from one scan to the other. As a consequence, after only three scans stainless steel exhibited better efficiency than platinum. It can be assumed that phosphate species adsorb in an irreversible way on platinum, which led to poisoning of the surface, while they can rapidly adsorb/desorb on/from stainless steel. A constant potential electrolysis performed at −1.1 V/SCE with a flat stainless steel electrode without stirring in 0.5 M phosphate/0.1 M KCl gave stable current around 13.5 A/m^2 for hours. It can be concluded that optimal exploitation of the deprotonation reaction of the phosphate species requires stainless steel to be used as the cathode material.

A calibration curve was recorded in 0.1 M KCl, 0.5 M phosphate pH 8.0, under galvanostatic conditions in order to avoid any possible disturbance due to potential control. The flow rate of the generated hydrogen was measured over periods of at least 15 min for each current value. An almost linear variation of the hydrogen generation rate (Q) was observed with the current density:

$$Q(mL/h/m^2) = 438.2 \, J \, (A/m^2)$$

This experimental correlation has been corrected by removing the 0.0316 atm partial pressure of water vapour (25 °C) that was unavoidably dragged by the hydrogen stream. Comparing to the theoretical correlation:

$$Q(mL/h/m^2) = (3600.V_{M25 \, °C})/(n.F) = 455.1 \, J \, (A/m^2)$$

where $V_{M25 \, °C}$ = 24400 mL/mole is the ideal gas molar volume at 25 °C, n = 2 the number of electron consumed per mole of produced hydrogen, and F the Faraday constant, gives a current efficiency value of 96%.

3.2. Microbial electrolysis cell

With the objective to assess the cathode efficiency, the MEC was designed to favour rate-limitation by the cathode. The total surface area of the stainless steel cathode (100 cm^2 taking both sides of the two 25 cm^2 plates into account) was 25 times smaller that the surface area of the graphite anode. Moreover, a cathode compartment with large volume was used to avoid variation in the composition of the bulk cathodic solution (particularly pH increase) during the successive electrolyses performed at different potential values. The cathode compartment was filled with a fresh solution of deionised water containing 0.5 M phosphate. At open circuit the cell voltage was approximately 0.2 V, i.e. only 70 mV from the thermodynamic value (0.131 V at pH 8.0). Voltage was applied from 0 to 2.0 V in
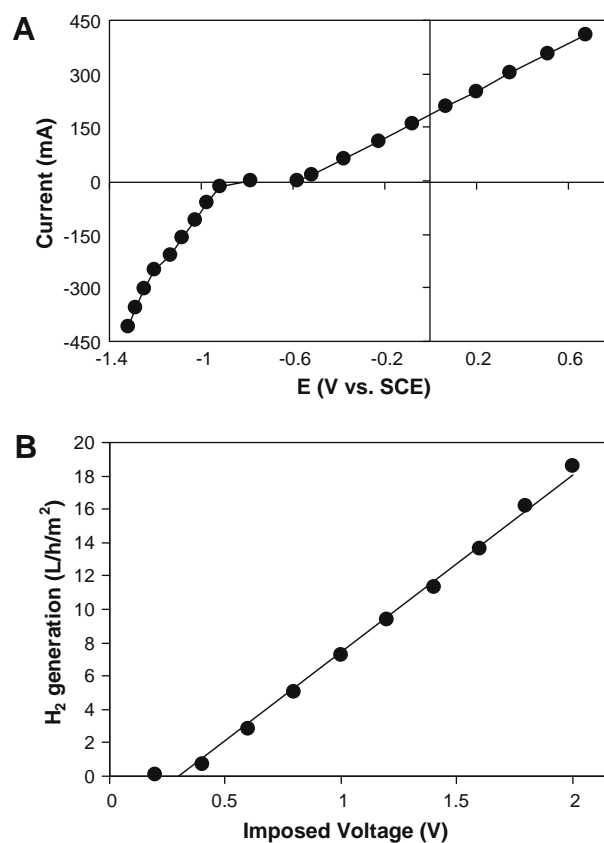

Fig. 3. Characterisation of a 25 L pilot MEC with 0.5 M phosphate pH 8.0 in the cathode compartment and seawater in the anode compartment. (A) Current–potential curves recorded by imposing successive cell voltages step by step; (B) hydrogen generation rate as a function of the cell voltage.

steps of 0.2 V. The current stabilised after less than 15 min at each potential step. Current values were plotted as a function of the anode potential and the cathode potentials measured with respect to the same reference electrode put in the anode compartment (Fig. 3A). Under 0.8 V applied voltage the cathode worked around −1.02 V/SCE and the anode at −0.22 V/SCE, sustaining current of 112 mA, i.e. 0.44 A/m^2 for the anode and 11.2 A/m^2 for the cathode. The anode gave modest performances compared to current densities up to 11 A/m^2 that have been reported with traditional MEC anodes formed from waste waters [15]. Nevertheless, anodes formed from waste waters are adversely affected by high salt concentration [1,15], which requires working with low conductivity and is the cause of the significant ohmic drop generally observed in MEC [16]. To our knowledge, this is the first time here that a microbial anode formed from marine sediments was implemented in a MEC. This anode operated with high salinity solution, here seawater, which allowed reducing drastically the internal resistance of the reactor and also possibly decreasing the methanogenesis side-processes.

The hydrogen flow rate, calculated with respect to the 100 cm^2 total surface area of the cathode, varied approximately linearly with the cell voltage (Fig. 3B). Under 0.8 V cell voltage, the hydrogen flow rate was 4.9 L/h/m^2 (11.2 A/m^2). Previous studies have generally reported lower values: 0.125 L/h/m^2 have been obtained with a platinum-coated titanium mesh under 0.5 V voltage [2], 2.97 L/h/m^2 have been reached under 0.85 V [17] and 2.5 L/h/m^2 under 0.9 V [7] with carbon paper enriched with platinum particles. Nevertheless, comparing cathode efficiencies with respect to the applied voltage only does not really make sense when different systems are considered, because the cathodes may work at different potentials depending on the ohmic drop, the anode kinetics

and the ratio of anode/cathode surface areas. The comparison of cathode efficiency should be done using similar cathode potentials, unfortunately such information are often difficult to extract from the data previously reported. According to a recent review [5] the best performance 5.2 L/h/m^2 [15] under 0.8 V was obtained with a carbon cloth cathode in a membraneless cell coupled to a very efficient carbon brush anode with a large surface area (314 times the cathode area) that allowed the cathode to work at -1.10 V vs. Ag/AgCl for a cell voltage of 0.8 V. Similar hydrogen production rates were obtained here in less optimal conditions, with the cathode working at only -1.02 V/ECS at 0.8 V voltage. The presence of a membrane with only 90 cm^2 total area might not ensure full exploitation of the whole anode surface area (0.25 m^2) and the setup with two flat cathodes (25 cm^2 each) may be detrimental to optimal assessment of the cathode performance. Nevertheless, the efficiency of the "phosphate/stainless steel" combination led to hydrogen generation rates that were of the same order than the best reported.

High concentrations of phosphate species in the cathode compartment may lead to significant diffusion to the anode compartment. The microbial anode must consequently keep its properties in the presence of phosphate species. Preliminary experiments that were performed with the microbial anode under constant polarisation at +0.2 V/SCE indicated no effect of 0.1 M phosphate concentration on the current recorded during several hours. It can consequently be hoped that this system could be implemented in a membrane-less MEC, as it has been proposed recently, replacing the membrane by a J-cloth [18]. Work is in progress in this direction.

4. Conclusion

The study demonstrated that a high concentration of phosphate species used in combination with a stainless steel cathode allowed high current density for hydrogen evolution in saline solutions at pH 8.0, a relevant pH value for MEC operation. The phosphate/stainless steel system was successfully applied in a MEC pilot, ensuring high hydrogen generation rates despite non-optimal design. This was also the first time that a microbial anode formed from marine sediment was used in a MEC. It is guessed that the high salinity used here may also help in controlling methanogenesis side-reactions. Further investigations are in progress in this direction.

References

[1] H. Liu, B. Logan, Environ. Sci. Technol. 39 (2005) 4317.
[2] R.A. Rozendal, H.V.M. Hamelers, G.J.W. Euveriknk, S.J. Metz, C.J.N. Buisman, Int. J. Hydrogen Energy 31 (2006) 1632.
[3] B.E. Logan, B. Hamelers, R. Rozendal, U. Schröder, J. Keller, S. Freguia, P. Aelterman, W. Verstraete, K. Rabaey, Environ. Sci. Technol. 40 (2006) 5181.
[4] B.E. Logan, Nat. Rev. Microbiol. 7 (2009) 375.
[5] B.E. Logan, D. Call, S. Cheng, H.V.M. Hamelers, T.H.J.A. Sleutels, A.W. Jeremiasse, R.A. Rozendal, Environ. Sci. Technol. 42 (2008) 8630.
[6] F. Harnisch, G. Sievers, U. Schröder, Appl. Catal., B-Environ. 89 (2009) 455.
[7] P.A. Selembo, M.D. Merrill, B.E. Logan, J. Power Sources 190 (2009) 271.
[8] D.F. Call, M.D. Merrill, B.E. Logan, Environ. Sci. Technol. 43 (2009) 2179.
[9] M.D. Merrill, B.E. Logan, J. Power Sources 191 (2009) 203.
[10] S. Da Silva, R. Basseguy, A. Bergel, Electrochim. Acta 49 (2004) 4553.
[11] L. De Silva Munoz, A. Bergel, R. Basseguy, Corr. Sci. 49 (2007) 3988.
[12] B. Erable, M.-A. Roncato, W. Achouak, A. Bergel, Environ. Sci. Technol. 43 (2009) 3194.
[13] S. Daniele, I. Lavagnini, M.A. Baldo, F. Magno, J. Electroanal. Chem. 404 (1996) 105.
[14] Dissociation Constants of Inorganic Compounds, in: D.R. Lide (Ed.), CRC Handbook of Chemistry and Physics, 87th ed., (Internet Version 2007), CRC Press/Taylor and Francis, Boca Raton, FL.
[15] D. Call, B.E. Logan, Environ. Sci. Technol. 42 (2008) 3401.
[16] T.H.J.A. Sleutels, H.V.M. Hamelers, R.A. Rozendal, C.J.N. Buisman, Int. J. Hydrogen Energy 34 (2009) 3612.
[17] H. Liu, S. Grot, B.E. Logan, Environ. Sci. Technol. 39 (2005) 4317.
[18] B. Tartakovsky, M.-F. Manuel, H. Wang, H.S.R. Guiot, Int. J. Hydrogen Energy 34 (2009) 672.